lncRNA UCA1 Functions as a ceRNA to Promote Prostate Cancer Progression via Sponging miR143

Yanlan Yu,[1] Fengbin Gao,[1] Qian He,[1] Gonghui Li,[1] and Guoqing Ding[1]

[1]Department of Urology, Sir Run Run Shaw Hospital, Zhejiang University School of Medicine, Hangzhou 310016, China

UCA1 (urothelial carcinoma associated 1) is a long non-coding RNA (lncRNA) that was found overexpressed in various human cancers including prostate cancer (PCa). However, the aspect of UCA1-miRNA-mRNA interaction in PCa remains unclear. In this study, we confirmed the role of UCA1 in PCa and found that UCA1 downregulation inhibited cell proliferation of PCa cells. Then we demonstrated that repressed UCA1 promoted the microRNA-143 (miR-143) expression and miR-143 could bind to the predicted binding site of UCA1. We then proved the anti-tumor role of miR-143 in PCa. Furthermore, we found that miR-143 displays its role in PCa via modulating the MYO6 expression. In summary, our study demonstrated that UCA1 exerts oncogenes activity in PCa, acting mechanistically by upregulating MYO6 expression through "sponging" miR-143.

INTRODUCTION

Prostate cancer (PCa) is the second most frequently diagnosed cancer in males worldwide.[1] With the development of prostate specific antigen (PSA) screening, MRI imaging, and new prostate biopsies protocols, detection of PCa has been increased.[2] Although radical prostatectomy and radiotherapy have improved the outcomes of localized PCa patients, the patients will develop metastatic castration-resistant prostate cancer (mCRPC), for which currently available treatment options have limited efficacy.[3,4] Therefore, it is important to investigate the molecular mechanisms and identify novel targets for the development of therapeutics for PCa patients.

As a type of non-coding RNA (ncRNA), long non-coding RNAs (lncRNAs) are molecules greater than 200 nt in length, frequently ranging up to 100 kb.[5] Several studies have attempted to uncover the mechanisms of lncRNAs in various human carcinomas. Increasing evidence has shown that altered expression level of lncRNAs contributed to cell proliferation and transformation of malignancies, including PCa.[6] Recently, a study reported that lncRNAs had also been implicated in resistance to chemotherapy.[7] Urothelial cancer associated 1, also known as UCA1, is located on 19p13.12 and encodes 3 isoforms (1.4, 2.2, and 2.7 kb) with poly(A) tails, which was first identified in human bladder carcinoma.[8] Previous studies had shown that overexpression of lncRNA UCA1 could promote tumor progression including PCa.[9] He et al.[10] found that UCA1 functions as a microRNA-204 (miR-204) sponge to upregulate CXCR4 expression in PCa. lncRNAs could act as competing endogenous

RNAs (ceRNAs) with microRNAs (miRNAs) to play a post-transcriptional regulatory role in the gene expression.[11] However, the aspect of UCA1-miRNA-mRNA interaction in PCa remains largely unknown.

Exosomes are small membrane-derived vesicles with a diameter of approximately 30–150 nm.[12] They play a crucial role in tumor proliferation and metastasis as mediators of cell-to-cell communication by transferring oncogenic molecules.[13] In general, most studies on tumor progression have focused on tumor cells themselves. Studies have shown that cancer cells can secrete exosomes, and lncRNAs have been found to be enriched and stable in exosomes.[14] In recent years, it has been shown that large intergenic non-coding RNA-p21 (lincRNA-p21) and several other lncRNAs are present in exosomes isolated from PCa patients.[15,16] In this study, we found that plasma exosomal UCA1 was obviously upregulated in PCa. Moreover, knockdown of UCA1 decreases cell growth by acting as a ceRNA of miR-143. We found that the UCA1-miR143-MYO6 regulatory network plays a key role in the development of PCa; highlighting this pathway may serve as a potential therapeutic target in PCa patients.

RESULTS

UCA1 Is Secreted by Exosomes into Serum of PCa Patients

In our current study, we collected abundant serums from 68 PCa patients and 50 normal people. After isolation of serum exosomes by sequential centrifugation, we characterized these vesicles with electron microscopy (Figure 1A). The nanoparticle tracking analysis (NTA) results showed a similar size distribution, and the peak size range was 80–135 nm (Figure 1B). Western blot analysis confirmed the presence of three well-known exosomal markers, CD63, TSG101, and Hsp 70 (Figure 1C). The qRT-PCR analyses showed that UCA1 was enriched in serum exosomes derived from PCa patients (Figure 1D).
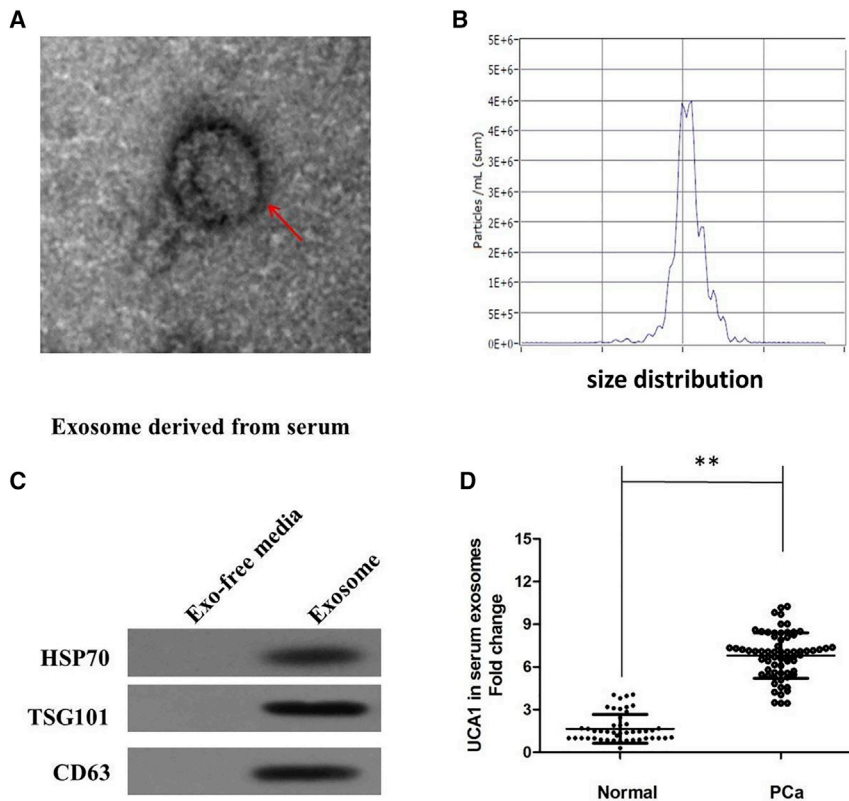
UCA1 Was Upregulated in Human PCa Tissues and Cell Lines

To identify the levels of UCA1 in PCa, we used qPCR assay to analyze the expression of UCA1 in 86 pairs of PCa tumor tissues. We first found that UCA1 was upregulated in PCa tissues when compared with normal tissues (p < 0.01; Figure 2A). Furthermore, UCA1

Figure 1. UCA1 is Secreted by Exosomes into Serum of PCa Patients

(A) Representative image of exosome (indicated by red arrows) derived from serum of PCa patients detected from electron microscopy. (B) NTA to determine the size distribution of exosome. (C) Western blot (WB) showing the expression of TSG101, CD70, and HSP70, which are the markers of exosome from purified serum exosome. (D) qRT-PCR for the abundance of UCA1 in serum exosomes. The levels of UCA1 in serum exosomes from PCa patients were significantly higher than that in normal individuals.

expression was significantly associated with advanced stage and metastasis (Table 1). To explore the expression of UCA1 in PCa cells, we performed qRT-PCR in various human PCa cell lines (DU145, PC-3, and LNCaP) and 22Rv1 cells and the human normal prostate epithelial cell line RWPE1. As shown in Figure 2B, UCA1 expression was higher in all PCa cells than in RWPE1 cells. Among PCa cells, DU145 cells showed the highest UCA1 level and the lowest expression of UCA1 was observed in 22RV1 cells.

UCA1 Promoted the Cell Proliferation of PCa *In Vitro*

To detect the role of UCA1 in PCa, we treated DU145 cells with small interfering UCA1 (si-UCA1) and treated 22RV1 cells with pcDNA-UCA1. si-UCA1 displayed a greatly inhibitory effect on UCA1 expression in DU145 cells, and UCA1 was overexpressed in 22RV1 cells transfected with pcDNA-UCA1 ($p < 0.01$; Figures 2C and 2D). To further determine the function of UCA1 on cell proliferation, it has been shown that downregulation of UCA1 significantly inhibited the cell proliferation of DU145 cells ($p < 0.01$; Figure 3A). In addition, compared with the pcDNA group, the cell proliferation of 22RV1 transfected with pcDNA-UCA1 was significantly increased ($p < 0.01$; Figure 3B).

Knockdown of UCA1 Promotes G1 Arrest and Causes Apoptosis in PCa *In Vitro*

Because UCA1 knockdown inhibited cell proliferation, we investigated whether UCA1 affects the cell cycle. The results from flow

cytometry showed that suppression of UCA1 in DU145 cells modulated the cell cycle by inducing G0/G1 arrest when compared with control group ($p < 0.01$; Figure 3C). Enhanced UCA1 expression increased the G2/M phase percentage of 22RV1 cells ($p < 0.01$; Figure 3D). In addition, to investigate whether apoptosis regulation was a potential contributing factor to the cell growth inhibition induced by knockdown of UCA1, an apoptosis assay was performed using flow cytometric analysis. The apoptotic percentage of UCA1-silenced DU145 cells was obviously increased ($p < 0.01$; Figure 3E). As expected, the cell apoptosis was markedly decreased in 22RV1 cells by pcDNA-UCA1 ($p < 0.01$; Figure 3F).

UCA1 Promotes PCa Tumorigenesis *In Vivo*

To determine whether UCA1 could affect tumorigenesis, we inoculated DU145 cells with stable UCA1 (sh-UCA1) and empty vector transfected DU145 cells into nude mice. Compared with the vector control, the tumor growth in the sh-UCA1 group was significantly slower ($p < 0.01$; Figure 4A). Remarkably, the average tumor weight was obviously lower in the sh-UCA1 group compared with the empty vector group ($p < 0.01$; Figure 4B). A qRT-PCR analysis of the UCA1 expression was then performed using the xenograft tumor tissues. The results showed that the levels of UCA1 expression in tumor tissues formed from sh-UCA1 cells were lower than those of the tumors formed in the control group ($p < 0.01$; Figure 4C).

UCA1 Inhibited miR-143 Expression

To investigate the effect of UCA1 on the expression of miRNAs, we applied the online software starBase v2.0 to predict the miRNAs that interacted with UCA1. The bioinformatics analysis revealed a potential combination of UCA1 and miR-143, the putative binding sites as shown in Figure 5A. In order to further validate the interaction, the UCA1 sequence containing the putative or mutated miR-143 binding site was cloned into the downstream of luciferase reporter gene, generating wild-type (WT)-UCA1 or mutant (MUT)-UCA1 luciferase reporter plasmids. Then the effect of miR-143 on WT-UCA1
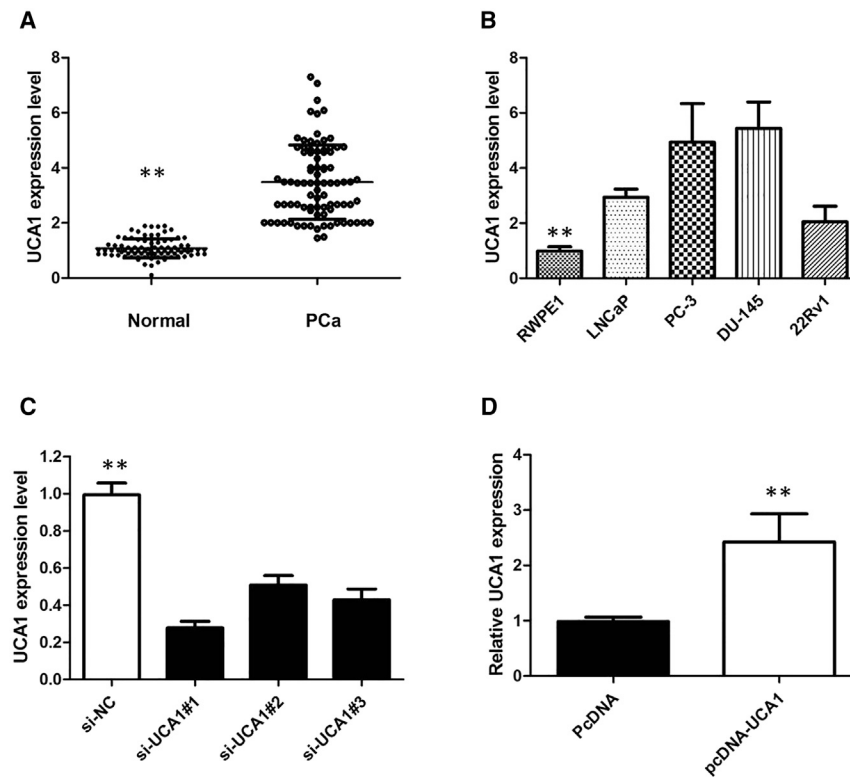
Figure 2. UCA1 was upregulated in human PCa tissues and cell lines

(A) qRT-PCR showing expression level of UCA1 in PCa tissues and adjacent noncancerous tissues. (B) qRT-PCR showing expression level of UCA1 in PCa cell lines. (C) UCA1 siRNAs were used to enhance efficiency of UCA1 knockdown in DU145 cells. (D) Ectopic overexpression of UCA1 by transfecting 22RV1 cells with pcDNA-UCA1 expression vector. All tests were performed at least three times. Data were expressed as mean ± SD. **p < 0.01.

miR-143 Inhibits PCa Progression by Targeting MYO6

To identify potential target genes of miR-143, we searched for candidate genes using TargetScan6.2 and miRBase miRNA databases. Bioinformatics analysis showed that miR-143 directly targets MYO6 (Figure 5D). To confirm the predictions, we conducted a WT or MUT MYO6 3′ untranslated region (UTR) luciferase reporter vector. MYO6-WT or MYO6-MUT was co-transfected with miR-143 mimics or negative control into HEK293T cells. The relative luciferase activity was remarkably reduced in cells co-transfected with the MYO6-WT luciferase reporter and miR-143 mimic than in the negative control cells. However, inhibitory effects were abolished when 3′ UTRs that contained both mutant-binding sites were co-transfected with miR-143, confirming that MYO6 is a target of miR-143 (p < 0.01; Figure 6A). Furthermore, the qRT-PCR was performed to detect the expression of miR-143 in PCa tissues and adjacent normal tissues. The miR-143 was significantly lower in PCa tissues compared with adjacent normal tissues (p < 0.01; Figure 6B). The immunohistochemistry results showed that MYO6 expression was significantly upregulated in PCa tissues compared with that in the adjacent normal tissues. MYO6 overexpression was observed in 62 of 86 (72.09%) PCa specimens when compared with adjacent normal tissues (17 of 86, 19.76%); the difference of MYO6 expression was statistically significant (p < 0.001; Figures 6C and 6D).

or MUT-UCA1 luciferase reporter systems was determined. The results showed that miR-143 mimic considerably reduced the luciferase activity of the WT-UCA1 luciferase reporter vector compared with negative control, while miR-143 mimic did not pose any impact on the luciferase activity of MUT-UCA1-transfected cells (p < 0.01; Figure 5B). In a further RNA immunoprecipitation (RIP) experiment, UCA1 and miR-143 simultaneously existed in the production precipitated by anti-AGO2 (p < 0.01; Figure 5C), suggesting that miR-143 is UCA1-targeting miRNA. These outcomes indicated that the interaction of UCA1 and miR-143 was recognized by the putative binding site.
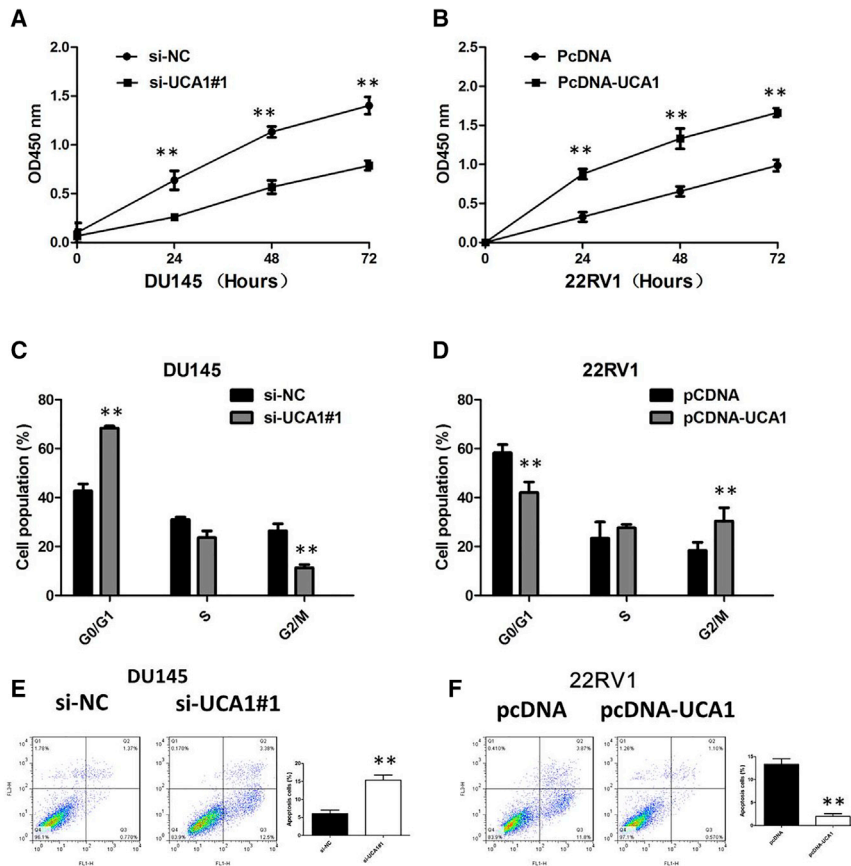
DISCUSSION

lncRNAs are a novel type of endogenous noncoding RNAs that regulate target gene expression by interacting with miRNA.[12,13] Emerging evidence shows that dysregulation of lncRNAs plays important roles in biological and pathological processes, including cancer development and progression. We herein uncover a novel carcinogenic role of UCA1 in the progression of PCa. We first found that UCA1 was significantly upregulated in the PCa tissues and PCa cell lines. Our subsequent studies demonstrate that UCA1 knockdown decreased cell proliferation, whereas UCA1 overexpression has the opposite results. In addition, UCA1 knockdown promoted significant arrest in the G0/G1 phase and an obvious increase in PCa cell apoptosis. These observations of tumor growth were verified in a mouse xenograft

Table 1. Correlation between UCA1 Expression and Clinicopathologic Characteristics of PCa Patients

Clinicopathological Features	Overall (n = 86)	UCA1 High (n = 43)	Low (n = 43)	p Value
Clinical T Stage				
T1 and T2	60	24	36	0.009
T3 and T4	26	19	7	
Lymph Node Metastasis				
Yes	21	16	5	0.01
No	65	27	38	
Distant Metastasis				
Yes	11	9	2	0.04
No	75	34	41	

Figure 3. Knockdown of UCA1 promotes G1 arrest and causes apoptosis in PCa in vitro

(A) CCK-8 assay showing knockdown of UCA1 inhibited cell proliferation of DU145 cells. (B) CCK-8 assay showing overexpression of UCA1 promoted cell proliferation of 22RV1 cells. (C) The flow cytometry assay showed that DU145 cells transfected with si-UCA1#1 had cell-cycle arrest at the G0/G1 phase in comparison with control cells. (D) The flow cytometry assay showed that 22RV1 cells transfected with pcDNA 3.1-UCA1 had cell-cycle arrest at the G2/M phase in comparison with control cells. (E) The flow cytometry assay showed that DU145 cells transfected with si-UCA1#1 had higher apoptotic rate in comparison with control cells. (F) The flow cytometry assay showed that 22RV1 cells transfected with pcDNA 3.1-UCA1 had lower apoptotic rate in comparison with control cells. All tests were performed at least three times. Data were expressed as mean ± SD. **$p < 0.01$.

has been identified as an oncogene, and it is usually highly expressed in a variety of cancers.[16] UCA1 was shown to activate Wnt/β-catenin signaling pathway to promote progression and epithelial-mesenchymal transition (EMT) in oral and breast cancer.[17,18] In gastric cancer, UCA1 has been shown as an early detection serum maker, and the induction of UCA1 by transforming growth factor β (TGF-β) leads to the enhanced invasion and migration in gastric cancer cells.[19] However, the expression and biological functions of UCA1 in PCa are poorly understood. In this study, we showed that overexpressed UCA1 was secreted by exosomes into the serum of PCa patients, suggesting that UCA1 might be a novel clinical molecular marker for PCa patients. Then, we reported that UCA1 expression was upregulated in PCa tissues and cell lines. Elevated expression of UCA1 was positively correlated with clinical T stage, lymph node metastasis, and distant metastasis. To further validate the expression level of UCA1 on tumor growth, we performed loss- and gain-of-function studies by knocking down or overexpressing UCA1 in two PCa cell lines, DU145 and

model. Specifically, lncRNA UCA1 acts as a sponge to sequester miR-143 from its target.

Significantly different lncRNA profiles can serve as phenotypic signatures for different cancers for their exploitation in cancer prognostics and therapeutics. Until now, different groups have screened the expression profile of lncRNAs in PCa tumors and found several disordered lncRNAs related to PCa carcinogenesis.[14,15] However, the underlying mechanisms are still not well understood. lncRNA UCA1
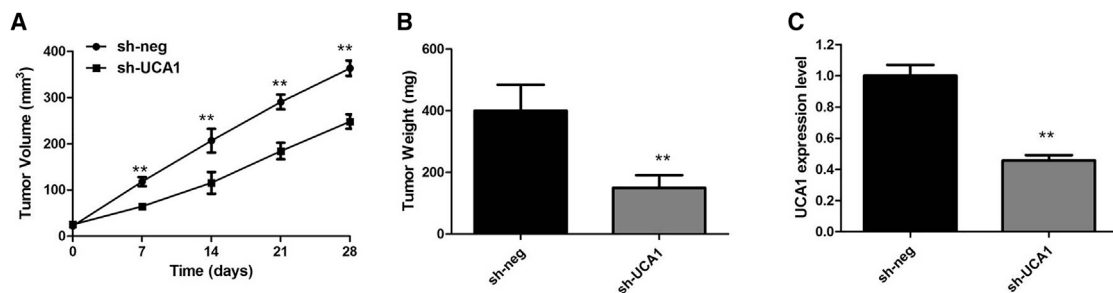
Figure 4. UCA1 promotes PCa tumorigenesis in vivo

(A) UCA1 knockdown inhibits DU145 tumor growth *in vivo*. The tumor volume curve of nude mice was measured. (B) The tumor weights of nude mice were measured. (C) The expression level of UCA1 in tumors of nude mice was detected by qRT-PCR. Data were expressed as mean ± SD. **$p < 0.01$.
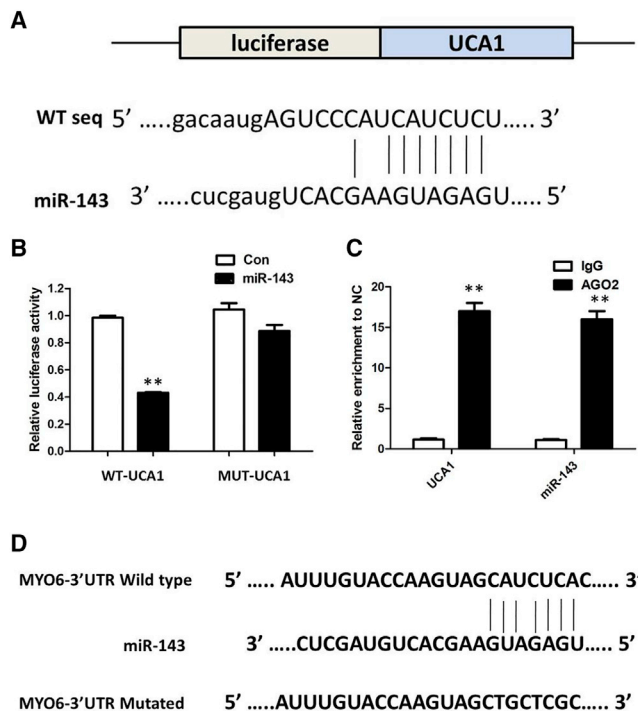
Figure 5. UCA1 inhibited miR-143 expression

(A) starBase v2.0 results showing the sequence of UCA1 with highly conserved putative miR-143 binding sites. (B) miR-143 mimic considerably reduced the luciferase activity of the WT-UCA1 luciferase reporter vector compared with negative control, while miR-143 mimic did not pose any impact on the luciferase activity of MUT-UCA1-transfected cells. (C) UCA1 and miR-143 simultaneously existed in the production precipitated by anti-AGO2. (D) Bioinformatics analysis revealed the predicted binding sites between MYO6 and miR-143. All tests were performed at least three times. Data were expressed as mean ± SD. **$p < 0.01$.

22RV1. Suppression of UCA1 significantly reduced the growth rate of DU145 cell lines compared with negative control-transfected cells. However, after overexpression of UCA1, the growth rate of 22RV1 cells was significantly increased compared to the control group.

A growing volume of literature has proposed that lncRNAs can act as ceRNAs, abrogating the endogenous suppressive effect of these miRNAs on their targeted transcripts. Bioinformatics analysis (star-Base 2.0, RNA22) of miRNA recognition sequences on UCA1 revealed the presence of more than 30 miRNAs binding sites. Among them, miR-143 stood out through detailed survey. To further confirm the underlying molecular mechanisms involved, we performed the RIP and luciferase assays and found the direct binding ability of the miR-143 response elements on the full-length UCA1 transcript. miR-NAs play crucial roles in the post-transcriptional regulation of gene expression by binding to the 3′ UTR of target mRNAs, thus inducing translation repression or degradation of mRNAs.[20] To date, miRNAs have been proved to play vital roles in cancer initiation and development, acting as either tumor suppressors or oncogenes.[21] In this study, we find that downregulation of miR-143 may play key roles

in the regulation of PCa. MYO6 was predicted as a downstream target of miR-143, which was confirmed by luciferase reporter assay. The aberrantly downregulated miR-143 accompanied by upregulated MYO6 may be potentially used for early diagnosis and determining prognosis in PCa patients.

Exosomes, derived from the endosomal compartment, are released in the extracellular milieu under various physiological and pathological conditions.[22] It has been reported that exosomes are closely related to tumor development,[23] but the role of cancer-secreted exosomal lncRNAs in PCa has not been clarified yet. Here, we performed transmission electron microscopy (TEM) to reveal the shapes and size of exosomes from serum of PCa patients. Notably, we found that the highly expressed UCA1 could be examined to serum exosomes of PCa patients.

In conclusion, this is the first study to investigate the regulatory function of UCA1 in PCa and the interaction between UCA1, miRNA, and MYO6. Through the UCA1/miR-143/MYO6 axis, UCA1 performed specific regulatory roles in the proliferation and progression of PCa. UCA1 could be a potential therapeutic target for PCa patients.

MATERIALS AND METHODS

Patients and Specimens

This study included 86 consecutive men diagnosed with PCa affirmed by clinical resection and pathology during 2010–2016. Cancer tissues and adjacent normal tissues surgically removed from PCa patients were immediately frozen in liquid nitrogen and stored at −80°C. For exosome purification, serum samples were collected from 68 PCa patients. The present research has been carried out in accordance with the World Medical Association Declaration of Helsinki and sanctioned by the Institutional Research Ethics Committee of Sir Run Run Shaw Hospital, Zhejiang University School of Medicine, and informed consent was signed by all 86 patients.

Isolation of Exosome

Serum and medium were filtered through a 0.45-μm pore polyvinylidene fluoride filter (Millipore, Billerica, MA, USA); subsequently, ExoQuick solution (System Biosciences, Mountain View, CA, USA) was added to serum and then incubated at room temperature for 0.5 h, and ExoQuick-TC solution was added to medium and then incubated at 4°C for 12 h, respectively. Exosome was collected by centrifugation at $1,500\times$ g for 30 min. Exosome pellets were resuspended in 25 μL PBS.

TEM

The sample of exosomes was diluted to 0.5 mg/mL by PBS. Subsequently, the specimen of exosomes was spotted onto a glow-discharged copper grid on the filter paper and then dried for 10 min using the infrared lamp. Finally, exosomes were stained with a drop of 1% aqueous solution of phosphotungstic acid for 5 min and then dried for 20 min using the infrared lamp. Exosomes were subsequently observed under a Hitachi H-7650 transmission electron microscope (Hitachi, Tokyo, Japan).
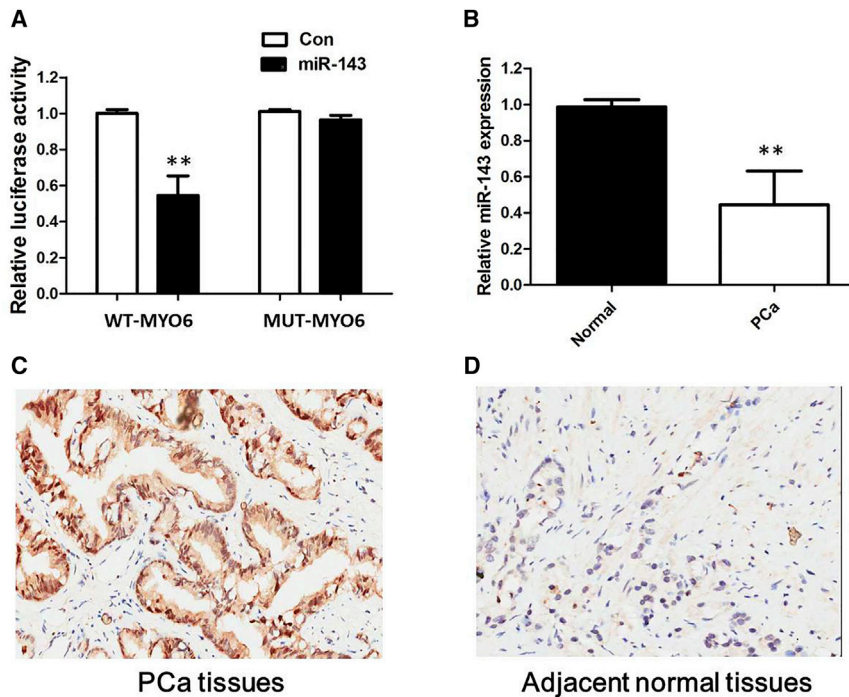
Figure 6. miR-143 inhibits PCa progression by targeting MYO6

(A) Luciferase reporter assay demonstrated that miR-143 mimics significantly decreased the luciferase activity of MYO6-WT in HEK293T cells. (B) miR-143 expression was significantly downregulated in PCa tissues compared with adjacent normal tissues by qRT-PCR analysis. (C and D) (C) Immunohistochemistry (IHC) analysis were performed to examine the expression levels of MYO in PCa tissues; (D) IHC analysis were performed to examine the expression levels of MYO in adjacent normal tissues. All tests were performed at least three times. Data were expressed as mean ± SD. **$p < 0.01$.

purchased from American Type Culture Collection (ATCC, Rockville, MD, USA). PCa cells were cultured in RPMI-1640 or Eagle's minimal essential medium, supplemented with 10% fetal bovine serum (FBS) and antibiotics. RWPE-1 was cultured in keratinocyte serum-free medium supplemented with 5 ng/mL human recombinant epidermal growth factor and 0.05 mg/mL bovine pituitary extract (Invitrogen, Carlsbad, CA, USA). Cultures were maintained in a 5% CO_2 humidified atmosphere at 37°C.

NTA

The size of exosomes was measured using a Nanosight NS 300 system (NanoSight Technology, Malvern, UK). Exosomes were re-suspended in PBS at a concentration of 5 μg/mL and further diluted 500- to 1,000-fold. Samples were manually injected into the sample chamber at room temperature. Each sample was configured with a 488 nm laser and a high-sensitivity sCMOS camera setting of 13 with an acquisition time of 30 s and a detection threshold setting of 7. At least 200 completed tracks were analyzed per video. Finally, the results were analyzed using NTA software.

Western Blotting

Total protein of exosome was extracted with radioimmunoprecipitation assay (RIPA) buffer (Sigma-Aldrich), and then the protein concentration was measured by bicinchoninic acid (BCA) assay (Pierce, Rockford, IL, USA). SDS-PAGE and western blot analyses were performed according to the standard procedures. The membranes and contents were probed using the following antibodies: anti-CD63 antibody (Abcam, Cambridge, UK), anti-TSG101 antibody (Abcam, Cambridge, UK), and anti-Hsp70 antibody (Cell Signaling Technology, Beverly, MA, USA). Secondary antibodies were F(ab)2 fragments of donkey anti-mouse immunoglobulin (Ig) or donkey anti-rabbit Ig linked to horseradish peroxidase (Jackson ImmunoResearch, USA). Immunoblotting reagents from an electrochemiluminescence kit were used (Amersham Biosciences, Uppsala, Sweden).

Cell Lines

PCa cell lines DU145, PC-3, LNCaP, 22Rv1, and the human nontumorigenic prostate epithelial cell line RWPE-1 were

RNA Isolation and qRT-PCR Assay

Total RNA was extracted and collected from PCa tissues or cells using the TRIzol reagent (Invitrogen) referring the instructions of manufacturer. First-strand cDNA was synthesized from 1 μg of total RNA by miScript reverse transcription kit (QIAGEN, Dusseldorf, Germany). The expression levels of UCA1 and miR-143 were quantified by miScript SYBR-Green PCR kit (QIAGEN). The relative fold change for gene expression was calculated using $2^{-\Delta\Delta CT}$ method, with GAPDH or U6 small nuclear RNA (snRNA) as internal control. The PCR primer sequences are as follows: U6 forward: 5′-CTC GCTTCGGCAGCACATATACT-3′, reverse: 5′-ACGCTTCACGAA TTTGCGTGTC-3′; UCA1 forward: 5′-CTCTCCTATCTCCCTTC ACTGA-3′, reverse: 5′-CTTTGGGTTGAGGTTCCTGT-3′; GAPDH forward: 5′-ACGGCAAGTTCAACGGCACAG-3′, reverse: 5′-GAC GCCAGTAGACTCCACGACA-3′.

Cell Transfection

Overexpressed UCA1 (pcDNA-UCA1) clones were based on the pcDNA-3.1 vector (Invitrogen). The UCA1 fragments were obtained by PCR and inserted into the XbaI/EcoRI sites. The constructs were identified and sequenced. The primers used were listed as follows: UCA1 forward primer F: 5′-CCGCTCGAGAGCGCGTGTGGC GGCCGAGCAC-3′, and UCA1 reverse primer R: 5′-CGCGGATCC AGACACGAGGCCGGCCACGCCACG-3′. Three specific siRNA targeting UCA1 (si-UCA1#1, si-UCA1#2, and si-UCA1#3) and scrambled siRNA control (si-NC) were obtained from GenePharma

(Shanghai, China). The sequences were described as follows: si-UCA1#1: 5′-GGACAACAGUACACGCAUAUU-3′; si-UCA1#2: 5′-GCCACCUACAUUAAAGCUAUU-3′; si-UCA1#3: 5′-GACCA GACCCUACCCGGUCAUUUAUUAUU-3′; miR-143 mimic (miR-143), scrambled mimic control (miR-NC), miR-143 inhibitor (anti-miR-143), and inhibitor control (anti-miR- NC) were purchased from RiboBio (Guangzhou, China). All these plasmids and oligonucleotides were transfected into cells by Lipofectamine 2000 reagent (Invitrogen) following the manufacturer's instructions.

Generation of UCA1 Stably Knocked Down Cell Line

The designed shRNA oligo targeting UCA1 and control oligo were cloned into pLKO.1 vectors to form pLKO.1-sh-UCA1 or pLKO.1-sh- NC plasmid, followed by co-transfected with pspAX2 and pMD2.G into 293T cells to produce sh-UCA1 or sh-NC lentivirus. Constructed sh-UCA1 or sh-NC lentivirus was respectively infected into DU145 cells, which were then screened with puromycin for over 7 days.

Cell Proliferation

Cell viability was determined by cell counting Kit-8 (CCK-8) assay. Different kinds of cells were seeded in 96-well plate with 5,000 cells/well. After 1, 2, and 3 days, cells were treated with CCK-8 reagent for 1 h in the incubator. Then optical density was detected by microplate reader at 450 nm in triplicate, and the mean value of absorbance was referred to the quantity of viable cells.

Flow Cytometry

The cells were harvested and were stained with Annexin V-FITC/PI (fluorescein isothiocyanate/propidium iodide) (KeyGEN Biotech, Nanjing, China) according to the instruction of the manufacturer. Then the cells were acquired by flow cytometry (FACScan, BD Biosciences, USA) and analyzed by FlowJo 7.6.1.

Cells for cell-cycle analysis were stained with propidium oxide by the CycleTEST PLUS DNA Reagent Kit (BD Biosciences) following the protocol and analyzed by FACScan. The percentage of the cells in G0-G1, S, and G2-M phase were counted and compared.

Tumor Xenograft Experiments

A total of 12 BALB/c male nude mice aged 3–4 weeks were purchased from the Experimental Animal Center of Zhejiang University. Cells were harvested and re-suspended in serum-free medium at a concentration of 1×10^7 cells/0.2 mL. Each mouse was inoculated subcutaneously in the right flank with cells stably transduced with shUCA1 or shControl. Tumor size was monitored every 7 days, and mice were euthanized after 4 weeks. This study was conducted according to the institutional guidelines of Sir Run Run Shaw Hospital, Zhejiang University School of Medicine and was approved by the institutional guidelines of Zhejiang University and by the Use Committee for Animal Care.

Luciferase Reporter Assay

Cells were cultured in 96-well plates and cotransfected with 50 nM miR-143 mimic (or NC), 50 ng of luciferase reporter vector (containing UCA1-WT, UCA1-MUT, MYO6 3′ UTR WT, or MYO6 3′-UTR MT), and 5 ng of Renilla luciferase plasmid using Lipofectamine 2000 (Invitrogen). Luciferase activity was measured using the dual-luciferase reporter assay system (Promega, Madison, WI, USA) after 48 h of incubation according to the manufacturer's instructions. Three independent experiments were performed in triplicate. Relative luciferase activity was normalized to the Renilla luciferase internal control.

RNA Immunoprecipitation Assay

RIP assay was performed using an EZ-Magna RiP Kit (Millipore, Billerica, MA, USA) in accordance with the manufacturer's instructions. Cells were lysed at 70%–80% confluence in RIP lysis buffer, and then incubated with magnetic beads conjugated with human anti-Ago2 antibody (Millipore) and normal mouse IgG control (Millipore) in RIP buffer. The RNAs in the immunoprecipitates were isolated with Trizol reagent and analyzed by qRT-PCR.

Immunohistochemistry

For each patient sample, three paraffin sections of 5 μm were prepared, one for H&E staining and the other two for immunohistochemical staining. PBS instead of primary antibodies was used for negative control, and the breast cancer tissue was used for positive control. Sections were dewaxed using xylene, followed by hydration with ethanol solutions and addition of EDTA for antigen retrieval. Later, sections were blocked with normal goat serum for 30 min to eliminate non-specific binding. Sections were incubated with anti-human MYO6 polyclonal antibody (1:1,000, ab124805; Abcam, Cambridge, MA, USA). Sections were then incubated with biotin-labeled secondary antibodies for 30 min at room temperature, followed by staining with diaminobenzidine (DAB). Finally, the sections were counterstained with hematoxylin. The result of staining was determined by two doctors who did not know the clinical condition of patients. The proportions of positive cells of 0%, 1%–5%, 6%–25%, 26%–75%, and 76%–100% were assigned with scores of 0, 1, 2, 3, and 4, respectively. Scores of 0–2 were considered as negative expression, and scores of 3–4 were considered as positive expression.

Statistical Analysis

Each experiment was repeated at least three times. Data are presented as mean ± SD. Student's t test was employed to dissect the differences between two groups, and one-way analysis of variance was used to determine the differences occurring between more than two groups. Statistical analyses were carried out with the use of SPSS 18.0 software (SPSS, Chicago, IL, USA), together with graphs generated using GraphPad Prism 6.0 (GraphPad Prism, San Diego, CA, USA). $p < 0.05$ was considered statistically significant.

Data Availability

The datasets used and/or analyzed during the current study are available from the corresponding author on reasonable request.

AUTHOR CONTRIBUTIONS

CONFLICTS OF INTEREST

The authors declare no competing interests.

ACKNOWLEDGMENTS

REFERENCES

1. Srigley, J.R., Amin, M., Boccon-Gibod, L., Egevad, L., Epstein, J.I., Humphrey, P.A., Mikuz, G., Newling, D., Nilsson, S., Sakr, W., et al. (2005). Prognostic and predictive factors in prostate cancer: historical perspectives and recent international consensus initiatives. Scand. J. Urol. Nephrol. Suppl. 216, 8–19.

2. Stephenson, A.J., Kattan, M.W., Eastham, J.A., Dotan, Z.A., Bianco, F.J., Jr., Lilja, H., and Scardino, P.T. (2006). Defining biochemical recurrence of prostate cancer after radical prostatectomy: a proposal for a standardized definition. J. Clin. Oncol. 24, 3973–3978.

3. Barlow, L.J., Badalato, G.M., Bashir, T., Benson, M.C., and McKiernan, J.M. (2010). The relationship between age at time of surgery and risk of biochemical failure after radical prostatectomy. BJU Int. 105, 1646–1649.

4. Guttman, M., and Rinn, J.L. (2012). Modular regulatory principles of large non-coding RNAs. Nature 482, 339–346.

5. Gutschner, T., and Diederichs, S. (2012). The hallmarks of cancer: a long non-coding RNA point of view. RNA Biol. 9, 703–719.

6. Sana, J., Faltejskova, P., Svoboda, M., and Slaby, O. (2012). Novel classes of non-coding RNAs and cancer. J. Transl. Med. 10, 103.

7. Wang, K.C., Yang, Y.W., Liu, B., Sanyal, A., Corces-Zimmerman, R., Chen, Y., Lajoie, B.R., Protacio, A., Flynn, R.A., Gupta, R.A., et al. (2011). A long noncoding RNA maintains active chromatin to coordinate homeotic gene expression. Nature 472, 120–124.

8. Xue, M., Chen, W., and Li, X. (2016). Urothelial cancer associated 1: a long noncoding RNA with a crucial role in cancer. J. Cancer Res. Clin. Oncol. 142, 1407–1419.

9. Li, F., and Hu, C.P. (2015). Long Non-Coding RNA Urothelial Carcinoma Associated 1 (UCA1): Insight into Its Role in Human Diseases. Crit. Rev. Eukaryot. Gene Expr. 25, 191–197.

10. He, C., Lu, X., Yang, F., Qin, L., Guo, Z., Sun, Y., and Wu, J. (2019). LncRNA UCA1 acts as a sponge of miR-204 to up-regulate CXCR4 expression and promote prostate cancer progression. Biosci. Rep. 39, BSR20181465.

11. Lin, C., Wang, Y., Wang, Y., Zhang, S., Yu, L., Guo, C., and Xu, H. (2017). Transcriptional and posttranscriptional regulation of HOXA13 by lncRNA HOTTIP facilitates tumorigenesis and metastasis in esophageal squamous carcinoma cells. Oncogene 36, 5392–5406.

12. Lee, B., Mazar, J., Aftab, M.N., Qi, F., Shelley, J., Li, J.L., Govindarajan, S., Valerio, F., Rivera, I., Thurn, T., et al. (2014). Long noncoding RNAs as putative biomarkers for prostate cancer detection. J. Mol. Diagn. 16, 615–626.

13. Cesana, M., Cacchiarelli, D., Legnini, I., Santini, T., Sthandier, O., Chinappi, M., Tramontano, A., and Bozzoni, I. (2011). A long noncoding RNA controls muscle differentiation by functioning as a competing endogenous RNA. Cell 147, 358–369.

14. Zhang, N., Li, Z., Bai, F., and Zhang, S. (2019). PAX5-induced upregulation of IDH1-AS1 promotes tumor growth in prostate cancer by regulating ATG5-mediated autophagy. Cell Death Dis. 10, 734.

15. Wu, X., Xiao, Y., Zhou, Y., Zhou, Z., and Yan, W. (2019). lncRNA SNHG20 promotes prostate cancer migration and invasion via targeting the miR-6516-5p/SCGB2A1 axis. Am. J. Transl. Res. 11, 5162–5169.

16. Fang, Z., Zhao, J., Xie, W., Sun, Q., Wang, H., and Qiao, B. (2017). LncRNA UCA1 promotes proliferation and cisplatin resistance of oral squamous cell carcinoma by sunppressing miR-184 expression. Cancer Med. 6, 2897–2908.

17. Wei, Y., Sun, Q., Zhao, L., Wu, J., Chen, X., Wang, Y., Zang, W., and Zhao, G. (2016). LncRNA UCA1-miR-507-FOXM1 axis is involved in cell proliferation, invasion and G0/G1 cell cycle arrest in melanoma. Med. Oncol. 33, 88.

18. Wang, Z.Q., He, C.Y., Hu, L., Shi, H.P., Li, J.F., Gu, Q.L., Su, L.P., Liu, B.Y., Li, C., and Zhu, Z. (2017). Long noncoding RNA UCA1 promotes tumour metastasis by inducing GRK2 degradation in gastric cancer. Cancer Lett. 408, 10–21.

19. Tuo, Y.L., Li, X.M., and Luo, J. (2015). Long noncoding RNA UCA1 modulates breast cancer cell growth and apoptosis through decreasing tumor suppressive miR-143. Eur. Rev. Med. Pharmacol. Sci. 19, 3403–3411.

20. Lin, P., Wen, D.Y., Li, Q., He, Y., Yang, H., and Chen, G. (2018). Genome-Wide Analysis of Prognostic lncRNAs, miRNAs, and mRNAs Forming a Competing Endogenous RNA Network in Hepatocellular Carcinoma. Cell. Physiol. Biochem. 48, 1953–1967.

21. Christensen, L.L., Holm, A., Rantala, J., Kallioniemi, O., Rasmussen, M.H., Ostenfeld, M.S., Dagnaes-Hansen, F., Øster, B., Schepeler, T., Tobiasen, H., et al. (2014). Functional screening identifies miRNAs influencing apoptosis and proliferation in colorectal cancer. PLoS ONE 9, e96767.

22. Thakur, B.K., Zhang, H., Becker, A., Matei, I., Huang, Y., Costa-Silva, B., Zheng, Y., Hoshino, A., Brazier, H., Xiang, J., et al. (2014). Double-stranded DNA in exosomes: a novel biomarker in cancer detection. Cell Res. 24, 766–769.

23. Dai, X., Chen, C., Yang, Q., Xue, J., Chen, X., Sun, B., Luo, F., Liu, X., Xiao, T., Xu, H., et al. (2018). Exosomal circRNA_100284 from arsenite-transformed cells, via microRNA-217 regulation of EZH2, is involved in the malignant transformation of human hepatic cells by accelerating the cell cycle and promoting cell proliferation. Cell Death Dis. 9, 454.